Energy deposition in N and N^+ by high-energy electron beams

Cite as: Journal of Applied Physics **64**, 982 (1988); https://doi.org/10.1063/1.341806
Submitted: 08 February 1988 . Accepted: 18 March 1988 . Published Online: 04 June 1998

R. D. Taylor, S. P. Slinker, and A. W. Ali

Energy deposition in N and N^+ by high-energy electron beams

R. D. Taylor,[a] S. P. Slinker, and A. W. Ali
Naval Research Laboratory, Washington, DC 20375-5000

(Received 8 February 1988; accepted for publication 18 March 1988)

A discrete, time-dependent energy deposition model is used to study high-energy electron-beam (100 eV–10 MeV) deposition in N and N^+. Both time-dependent and steady-state secondary electron distributions are computed. The loss function, mean energies per electron-ion pair production (W), production efficiencies, and distribution functions are presented for a wide range of energies. The latest experimental and theoretical cross sections are used in the model which predicts that W is approximately 31 eV for N and 72 eV for N^+ over a wide range of beam energies. The sensitivity of these results to assumed background ionization fractions is also investigated.

I. INTRODUCTION

The problem of electron energy deposition in gases has been the subject of detailed study for over thirty years. Its importance to different areas of physics is well known. The interaction of radiation with matter[1,2] and biological systems[3] are two areas where early progress was made. Subsequently, deposition problems played a role in the study of the precipitation of energetic electrons in the upper atmosphere and auroral emissions.[4-7] Currently, energy deposition is of interest in research of electron beams, including electron-beam propagation in the atmosphere,[8-11] electron-beam-generated lasers,[12-14] and electron-beam-generated discharges and their diagnostics.[14] Detailed deposition calculations generally provide information on the secondary electron distribution, primary and secondary electron excitation rates for the internal modes of the atoms or molecules, total ionization rate, and the mean energy expended by an electron in generating an electron-ion pair. The mean energy W is often used to provide a simple description of the cumulative ionization of the gas by high-energy beam electrons, i.e., the creation of secondaries, tertiaries, etc.

In a previous paper[10] (denoted by I), we reported on the development of a new electron energy deposition code and its application to the study of deposition in atomic oxygen. While extensive work[1-22] has been done on the study of deposition in air and gases such as O, O_2, N_2, H_2, Ar, and He, among others, minimal effort[11] has been made for N or N^+. Since both of these species are present following the dissociation and ionization of air by long, pulsed, intense electron beams, they merit further study. Here, results are presented and discussed for electron-beam energy deposition in N and N^+ for beam energies between 100 eV and 10 MeV. Results are obtained using the deposition code mentioned above.[10] In particular, secondary electron distributions are obtained by solving a time-dependent Boltzmann equation. These distribution functions relax to steady-state results from which yield spectra, production efficiencies of specific states, energy partitioning, and W are computed. Loss functions are also computed and compared to Bethe's relativistic equation.[23] Results which are specific to beam deposition in N and N^+ are presented. General results are not discussed in detail since many of the resulting conclusions are identical to those presented in paper I. For example, examinination of $\Phi(T)$ [defined in Eq. (27) in paper I] showed the continuous-slowing-down approximation (CSDA) to be valid for energies greater than 1 keV. Analysis of the same quantity for deposition in N and N^+ gives nearly the same result and need not be elaborated on further.

The Boltzmann equation and the specific nitrogen models are given in Sec. II. This includes a discussion of the electron-impact excitation and ionization cross sections used in the deposition scheme. The numerical techniques implemented in the calculation were described in detail in the Appendix of paper I. Results are presented and discussed in Sec. III. Summary remarks are reserved for Sec. IV.

II. THE SECONDARY ELECTRON DISTRIBUTION

Some of the information presented in this section was also presented in Sec. II of paper I. Here, specific N and N^+ cross-section information is discussed in detail.

The secondary electron distribution for a spatially homogeneous electron beam impinging upon a gas is obtained by solving

$$\frac{\partial f}{\partial t}(T,t) = S(T,t) + \sum_s N_s(t)\Bigg[\sum_j \left[\sigma_{sj}(T+E_{sj})v(T+E_{sj})f(T+E_{sj},t) - \sigma_{sj}(T)v(T)f(T,t)\right] + \sum_i \Bigg(\int_{T+I_{si}}^{2T+I_{si}} d\epsilon\, \sigma'_{si}(\epsilon,\epsilon-I_{si}-T)v(\epsilon)f(\epsilon,t) + \int_{2T+I_{si}}^{T_m} d\epsilon\, \sigma'_{si}(\epsilon,T)v(\epsilon)f(\epsilon,t) - \sigma_{si}(T)v(T)f(T,t)\Bigg)\Bigg] + N_p(t)\frac{\partial}{\partial t}\left[L_p(T)v(T)f(T,t)\right], \quad (1)$$

[a] Present address: Berkeley Research Associates, P. O. Box 852, Springfield, VA 22150.

 0021-8979/88/150982-12$02.40

where $f(T,t)$ is the secondary electron density (cm^{-3} eV^{-1}) for electrons with kinetic energy T and speed $v(T)$, $S(T,t)$ is the production rate ($cm^{-3}\,s^{-1}\,eV^{-1}$) due to the incident electron beam, T_m is the maximum secondary electron energy, $N_s(t)$ is the number density of species s, $N_p(t)$ is the plasma electron number density, and $L_p(T)$ is the loss function of a secondary electron with energy T to the plasma electrons. The effects of electron-electron collisions are frequently modeled by loss functions such as $L_p(T)$.[4,8,10,24] Inelastic and ionizing collisions are accounted for by using detailed cross sections. For example, $\sigma_{sj}(T)$ is the jth electron impact excitation cross section for species s where E_{sj} is the excitation energy. For ionization channel i, the total ionization cross section is $\sigma_{si}(T)$, I_{si} is the ionization potential, and $\sigma'_{si}(\epsilon,T)$ is the differential ionization cross section for an incident electron with energy ϵ producing an additional electron with energy T.

Equation (1) assumes that the electric and magnetic field effects due to the beam are negligible. Although elastic and superelastic collisions between the electrons and background gas are neglected, they may be incorporated in a straightforward way. Furthermore, in this paper, we consider the case of a single component background gas (either N or N^+) and assume that both the gas density ($N_s = N_0$) and source term are time independent. In the following sections, the species index, s, is dropped. For deposition in N, the atoms initially reside in the $^4S^0$ (ground) state. Energy loss to the $2p^3\,^2D^0$ and $2p^3\,^2P^0$, all $n = 3$ states, one specific Rydberg series ($n \geqslant 4$) state, and the $^3P\,N^+$ state is accounted for. For deposition in N^+, the atoms initially reside in the ^3P (ground) state. Energy loss to the $2p^2\,^1D$ and $2p^2\,^1S$, all $n = 3$ states, three specific Rydberg series ($n \geqslant 4$) states, and the $^2P^0\,N^{++}$ state is described by the model. The assumption that the background gas density is time independent is based on assuming that the accumulation of products is small compared to the original population of the gas. In a situation where N and N^+ are produced in significant amounts, contributions from the $N^2D^0 2p^3$ state and the $N^{+1}D\,2p^2$ should also be included. However, we have considered deposition from the ground state only, as a first step, in order to simplify the calculation. Extending the results is straightforward and shall be the subject of future investigation.

Within the context of the above assumptions and this model, the various terms appearing in Eq. (1) are discussed in detail below. Analytic forms for the relevant excitation and ionization cross sections are presented in Secs. II B thru II E. A detailed discussion of these forms, their reduction to well-known theoretical results, and their relative accuracy in comparison to existing measurements and calculations is given elsewhere.[25]

A. The source term $S(T,t)$

The emphasis in this paper is on high-energy electron-beam deposition in a single component gas, i.e., N or N^+. Beam electrons are assumed to make at most one collision and then leave the area of interest. The source term for the generation of the secondary electrons is

$$S(T,t) = S(T) = N_0 N_b(T_b) v(T_b) \sum_i \sigma'_i(T_b,T), \quad (2)$$

where $N_b(T_b)$ is the number density of beam electrons whose energy is T_b, $\sigma'_i(T_b,T)$ is the differential ionization cross section for producing a secondary electron with energy T [restricted to energies $\leqslant (T_b - I_i)/2$], and the time independence is made explicit. The exact form of the differential cross section is discussed in Sec. II D.

When energetic electrons do not leave the area of interest, but are completely stopped by the medium, the source term may be given by

$$S(T,t) = S(T) = N_1 \delta(T - T_b), \quad (3)$$

where N_1 is the number of completely stopped electrons per cm^3 per s. This case is not treated in this paper, but is discussed in paper I as is the relationship between this work and the pioneering work of Spencer and Fano.[2]

B. Electron impact excitation cross sections: Nitrogen atom

Electron-impact excitations of nitrogen are either optically (dipole) allowed or optically forbidden. The cross section for optically allowed transitions from the ground state to an excited state j is given by,

$$\sigma_j = A_j \frac{4\pi a_0^2 R^2 f_j}{E^2}\left(\frac{E}{E_j} - 1\right) \times \left[\ln\left(\frac{4C_j E}{E_j}(1-\beta^2)^{-1}\right) - \beta^2\right], \quad (4)$$

where πa_0^2 is the atomic unit cross section (0.88×10^{-16} cm^2), R is the hydrogen atom ionization potential (13.60 eV), E_j is the transition energy, f_j is the optical oscillator strength, A_j and C_j are adjustable parameters, and $\beta = v/c$, where v is the electron velocity. The energy E is $mv^2/2$ where m is the electron rest mass. For energies less than 10^4 eV, E is approximately equal to the electron kinetic energy, T; relativistic effects begin to play a role above that value. Equation (4) accounts for the threshold behavior in a manner first proposed by Drawin[26] and includes the energy dependence expected according to the relativistic Bethe formula based on the Born approximation.[27,28] It is reasonable to use this form for energies up to 10^9 eV. Above that energy, coupling to the radiation field cannot be neglected. The parameters used in Eq. (4) for optically allowed transitions are given in Table I. The oscillator strengths were taken from Wiese, Smith, and Glennon.[29]

TABLE I. Electron-impact excitation cross-section parameters for optically allowed N and N^+ transitions.

	N parameters			
State	E_j	A_j	C_j	f_j
^4P3s	10.33	1.0	0.3125	0.130
$^4P2p^4$	10.92	1.0	0.3125	0.350
	N^+ parameters			
State	E_j	A_j	C_j	f_j
$^3D^0 2p^3$	11.42	1.0	0.3125	0.170
$^3P^0 2p^3$	13.52	1.0	0.3125	0.220
$^3P^0 3s$	18.45	1.0	0.3125	0.089
$^3S^0 2p^3$	19.21	1.0	0.3125	0.230
$^3D^0 3d$	23.22	1.0	0.3125	0.260
$^3P^0 3d$	23.39	1.0	0.3125	0.082

In atomic nitrogen, transitions to forbidden states are categorized as those involving (1) the $2p^3\ ^2D^0$ and $2p^3\ ^2P^0$ states and (2) higher-lying Rydberg states. Generally, these transitions proceed because of existing electric quadrupole moments or electron exchange effects. Cross sections for electron-impact excitation of such transitions do not display the characteristic $E^{-1} \ln E$ behavior at high energies, but instead decrease more rapidly.[30] To describe such transitions, we adopt a form used extensively by Green and coworkers,[19,31–35]

$$\sigma_j = A_j [4\pi a_0^2 R^2/(EE_j)^a][1-(E_j/E)^b]^c, \tag{5}$$

where a, b, c, and A_j are parameters and the other quantities are defined above. Equation (5), with the proper choice of parameters, reduces to well-known theoretical results.[25] Table II gives the parameters for collisional excitation of the $2p^3\ ^2D^0$ and $2p^3\ ^2P^0$ states. Two sets of parameters were used to model these cross sections. These give good agreement with existing experimental[36] and theoretical[37–39] results. Our preference for using two sets of parameters is that the desired E^{-3} high-energy behavior[25,26,37] can be maintained.

Electron-impact excitation cross sections for transitions to high-lying excited states are obtained using the general procedure developed by Green and Dutta.[32] Setting $b=1$ and rewriting Eq. (5) to correspond to their form, the cross section is given by

$$\sigma_j = c_j f_j \frac{4\pi a_0^2 R^2}{E_j^2}\left(1-\frac{E_j}{E}\right)^c\left(\frac{E_j}{E}\right)^a. \tag{6}$$

The oscillator strength, f_j, is defined as

$$f_j = f^*/(n-\rho)^3, \tag{7}$$

where ρ (the quantum defect) and f^* are assumed constant within a Rydberg series and ρ is determined from

$$E_j = I_j - R/(n-\rho)^2. \tag{8}$$

In principle, the value of f^* is obtained by equating f_j with the known oscillator strength of an optically allowed transition in the series. As an alternative, the parameters c_j, a, c,

TABLE II. Electron-impact excitation cross-section parameters for N $^2D^0$ and $^2P^0$ transitions.

	N parameters					
State	E_j	A_j	a	b	c	
$^2D^0 2p^3$	2.38	0.025	1	1	1	$\leqslant$40.0 eV
		227.72	3			$>$ 40.0 eV
$^2P^0 2p^3$	3.57	0.0175	1	1	1	$\leqslant$ 40.0 eV
		356.04	3			$>$ 40.0 eV

TABLE III. Electron-impact excitation cross-section parameters for N and N^+ Rydberg-state transitions.

	N parameters				
State	E_j	c_j	f_j	a	c
^2P3p	10.68	0.40	0.150	2	1
$^2S^0 3p$	11.60	0.30	0.191	2	1
$^4D^0 3p$	11.75	0.10	0.130	1	1
$^4P^0 3p$	11.84	1.50	0.130	0.7	2.5
$^4S^0 3p$	11.99	0.07	0.150	0.7	0.5
$^2D^0 3p$	12.00	0.14	0.140	2	1
$^2P^0 3p$	12.12	0.40	0.150	2	1
$^2D3s'$	12.35	...	...	...	...
^2P3d	12.97	0.40	0.150	2	1
^4F3d	12.98	0.10	0.130	1	1
^2F3d	12.99	0.14	0.140	2	1
^4P3d	12.99	1.50	0.130	0.7	2.5
^4D3d	13.01	0.10	0.130	1	1
^2D3d	13.03	0.14	0.140	2	1
$^2D^0 3p'$	13.70	...	...	...	...
$^2F^0 3p'$	13.72	...	...	...	...
$^2P^0 3p'$	13.92	...	...	...	...
$^2S3s''$	14.41	...	...	...	...
$^2G3d'$	14.89	...	...	...	...
$^2S3d'$	14.94	...	...	...	...
	N^+ parameters				
State	E_j	c_j	f_j	a	c
$^1D^0 2p^3$	17.86	0.40	0.210	2	1
$^1P^0 3s$	18.47	0.30	0.110	2	1
^{1}P3p	20.39	0.30	0.110	2	1
^3D3p	20.63	1.50	0.077	0.7	2.5
$^1P^0 2p^3$	20.65	0.30	0.310	2	1
^3S3p	20.92	1.50	0.077	0.7	2.5
^3P3p	21.13	0.07	0.089	0.7	0.5
^1D3p	21.57	0.40	0.089	2	1
^1S3p	22.08	0.40	0.089	2	1
$^3F^0 3d$	23.11	0.10	0.077	1	1
$^1D^0 3d$	23.17	0.40	0.089	2	1
$^1F^0 3d$	23.45	0.14	0.083	2	1
$^1P^0 3d$	23.55	0.30	0.110	2	1

and ρ may be chosen according to the criteria proposed by Jusick *et al.*[40] Dalgarno and Lejeune[4] and Slinker, Taylor, and Ali[10] used this method for oxygen, letting f^* vary only according to which ionization continuum the series belonged to. Adopting this approach, the parameters for all $n = 3$ states included in this calculation are presented in Table III. For the ^3P continua, $f^* = 3.475$. We have not included states which ionize to the ^1D or ^1S continua.

Energy loss to Rydberg states with $n>4$ and belonging to a series containing one of the allowed transitions given in Table I are also modeled by Eq. (6). The effective f_j is obtained by solving Eq. (8) for ρ (E_j is the energy of the $n = 4$ state) and integrating Eq. (7) from $n = 4$ to ∞. $\bar{E}_j$ (the average of E_j and I_j) is used in Eq. (6) in place of E_j. Parameters are given in Table IV.

C. Electron impact excitation cross sections: Nitrogen ion

In the nonrelativistic limit, Eq. (4) can be written as

$$\sigma_j = (8\pi/\sqrt{3})(R^2/EE_j) f_j g_j \pi a_0^2, \tag{9}$$

where g_j is an effective Gaunt factor given by

$$g_j = A_j \frac{\sqrt{3}}{2\pi}\left(1 - \frac{E_j}{E}\right)\ln\left(\frac{4E}{E_j} C_j\right). \tag{10}$$

Equation (9) is a standard form for the excitation cross section subject to the Born–Bethe approximation which is valid at high energies where distant encounters are most important and short-range interactions between the free and atomic electrons can be neglected. Equation (10) is a form for the effective Gaunt factor proposed by Drawin,[26] which modifies the cross section so as to account for low-energy collisions in a simple way.

For neutrals, the Born approximation assumes that the perturbing electron is represented by plane waves. Positive ions, however, introduce an ion field which causes a distortion of the plane waves. At high energies, this distortion is negligible and the ion behaves like a neutral. However, at low energies it must be accounted for and Eq. (4) [or Eq. (9)] should be modified to be of use. Van Regemorter[41] and Seaton[42] deduced that the effective Gaunt factor in the semiempirical formula given by Eq. (9) is approximately constant near threshold. Vainstein's[43] distorted-wave calculations for carbon ions and the hydrogenic results of Burgess[44] provided justification for choosing a value of 0.2. Analogously, the nonrelativistic limit of Eq. (4) is given by Eq. (9) where g_j is now defined as

$$g_j = \begin{cases} 0.2, & E < E_{cj} \\ A_j \dfrac{\sqrt{3}}{2\pi} \ln\left(\dfrac{4E}{E_j} C_j\right), & E > E_{cj}, \end{cases} \tag{11}$$

where E_{cj} is chosen to ensure continuity. According to Eqs. (9) and (11), the cross section is peaked at threshold.[26] Relativistic corrections are then included in the manner of Eq. (4).

Electron-impact excitation cross sections for optically allowed transitions are computed as discussed above. Parameters for the relevant transitions are given in Table I. Again, oscillator strengths were obtained from Wiese and co-workers.[29] While there are no experimental results to compare with, Ganas[45] has used the Born approximation to calculate the generalized oscillator strength, and from that the cross section, for the $^3P \rightarrow {}^3P^0$ 672-Å transition. A comparison[25] between his calculation and the above approach shows that the effect of the constant Gaunt factor in the threshold regime is pronounced. For higher impact energies agreement is good.

The cross section for transitions from the ground state to the $2p^3\ ^1D$ and $2p^3\ ^1S$ states is given by

$$\sigma_j = [(1.197\times 10^{-15})/g_i E]\,\Omega_j, \tag{12}$$

where g_i is the initial state statistical weight ($g_i = 9$) and Ω_j is the collision strength for the final state. No experimental measurements of these cross sections exist, so Eq. (12) is used along with collision strengths calculated by Henry, Burke, and Sinfailam,[37] which are in good agreement with those calculated previously by Saraph, Seaton, and Shemming.[46] In the present calculations, the variation of the collision strength with energy is neglected. This leads to a slight underestimate of the cross section.

To describe energy loss to $n = 3$ Rydberg states, Eq. (6) is used with the parameters given in Table III. These parameters are also chosen according to the criteria of Jusick *et al.*[40] In Eq. (7), $f^* = 1.34$ for states with an outer shell configuration of $2s2p^3$, while $f^* = 2.06$ for the other states. Although the ion cross sections should be finite at threshold, Eq. (6) has been used as given. Table IV gives the parameters used in Eq. (6) to account for Rydberg states with $n\geqslant 4$ in the manner discussed above.

TABLE IV. Electron-impact excitation cross-section parameters for N and N^+ Rydberg series ($n>4$) transitions.

	N parameters				
State	$\bar{E}_j$	c_j	f_j	a	c
^4Pns	13.70	1.50	0.109	0.7	2.5
	N^+ parameters				
State	$\bar{E}_j$	c_j	f_j	a	c
$^3P^0ns$	26.98	0.07	0.036	0.7	0.5
$^3D^0nd$	27.82	1.50	0.032	0.7	2.5
$^3P^0nd$	27.85	0.07	0.036	0.7	0.5

D. Electron ionization cross sections: Nitrogen atom

The total ionization cross section is given, analogous to Eq. (4), by

$$\sigma_i = A_i \frac{4\pi a_0^2 R^2}{E^2}\left(\frac{E}{I_i} - 1\right)\left[\ln\left(\frac{4C_i E}{I_i}(1-\beta^2)^{-1}\right) - \beta^2\right]. \tag{13}$$

Equation (13) reduces identically to the Drawin formula[26] for low energies, displays the desired $E^{-1}\ln E$ behavior at high energies, and shows the expected rise for relativistic energies.

The differential ionization cross section, $\sigma_i'(T,\epsilon)$, is given by[22,25]

$$\sigma'(T,\epsilon) = \frac{\sigma(T)}{\tan^{-1}[(T-I)/2b(T)]}\frac{b(T)}{b(T)^2+\epsilon^2}, \quad (14)$$

for the low energy regime, defined here as $T<I_i+10$ eV. The index i has been dropped for convenience. When $T>I_i+10$ eV then

$$\sigma'(T,\epsilon) = [\sigma(T)b(T)/p(T)]g(T,\epsilon), \quad (15)$$

where

$$g(T,\epsilon) = \frac{1}{(T+mc^2)^2} - \frac{(2Tmc^2+m^2c^4)}{(T+mc^2)^2} \times \frac{1}{[b(T)+\epsilon][b(T)+T-\epsilon-I]} + \frac{1}{b(T)^2+(T-\epsilon-I)^2} + \frac{1}{b(T)^2+\epsilon^2}, \quad (16)$$

and

$$p(T) = \tan^{-1}\left(\frac{T-I}{b(T)}\right) - \frac{b(T)}{T+2b(T)-I}\frac{(2Tmc^2+m^2c^4)}{(T+mc^2)^2} \times \ln\left(\frac{b(T)+T-I}{b(T)}\right) + \frac{b(T)(T-I)}{2(T+mc^2)^2}. \quad (17)$$

In Eqs. (14)–(17), $b(T)$ is an energy-dependent parameter and mc^2 is the electron rest-mass energy (0.511 MeV). As above, T is the kinetic energy of the incident electron (primary) and ϵ the outgoing (secondary) electron. Equation (17) ensures that when the secondary electron is defined as the least energetic of the two, then

$$\sigma_i(T) = \int_0^{(T-I_i)/2} \sigma_i'(T,\epsilon)\,d\epsilon. \quad (18)$$

The parameters A_i and C_i have been chosen so that Eq. (13) provides a compromise fit to the recent calculations of McGuire[47] and experimental measurements of Brook, Harrison, and Smith.[48] Additional theoretical and experimental results are discussed in detail elsewhere.[25] Since transitions to $N^+(^1D)$ and $N^+(^1S)$ do not occur in photoionization and, therefore, are expected to have small collision cross sections, they are neglected in this study. The parameter $b_i(T)$ is assumed to have the form

$$b_i(T) = \begin{cases} b_{i0} & \text{for } T \leqslant \exp(k_i) \\ (b_{i0}k_i)/\ln T & \text{for } T \geqslant \exp(k_i), \end{cases} \quad (19)$$

where b_{i0} and k_i are constants. The ionization parameters are given in Table V. From the oxygen work,[10] we found that b_{i0} is approximately equal to the ionization potential. The functional form of $b_i(T)$ at higher energies and the value of k_i are chosen so that the loss function, $L(T)$ (discussed below), is in agreement with Bethe's relativistic formula.[23]

Equations (13)–(19) are used because they give a good accounting of ionization for impact energies ranging from threshold to relativistic, are easily fit to available experimental or theoretical data, include exchange and spin-dependent effects, and result in a loss function which agrees with Bethe's formula in the appropriate limit. There are, however, alternative forms which may be used. For example, Inokuti *et al.*[49] present an expression, based on a polynomial fit to the generalized oscillator strength per unit energy range, which they use to model secondary electron spectra resulting from proton impact on various molecules. Porter, Jackman, and Green[19] use a form similiar to the equations above, in lieu of an expression derived from the generalized oscillator strength, to examine deposition in N_2 and O_2 by relativistic electrons and protons.

TABLE V. Electron-impact N and N^+ ionization cross-section parameters.

	N parameters			
Final state	A_i	C_i	b_{i0}	k_i
$N^+(^3P)$	2.20	0.25	15.0	7.40
	N^+ parameters			
Final state	A_i	C_i	b_{i0}	k_i
$N^{++}(^2P^0)$	2.00	0.39	29.6	9.59

E. Electron ionization cross sections: Nitrogen ion

The ionization parameters used in Eqs. (13)–(19) are given in Table V. A_i and C_i were chosen to match the total ionization cross sections measured by Harrison, Dolder, and Thonemann.[50] These data also agree, to within 20%, with the calculations of McGuire.[51] A comparison between these and additional experimental and theoretical results is presented elsewhere.[25] Again, $b_i(T)$ and k_i were chosen to ensure agreement between $L(T)$ and Bethe's relativistic loss formula.

F. Energy loss to plasma electrons

Perkins[52] has derived the rate of energy loss to plasma electrons by a test electron. These results have been utilized by Schunk and Hayes[24] to obtain expressions for the energy loss for nonrelativistic energies. For relativistic energies, the energy loss is given by Tsytovich.[53] In Eq. (1), these results are used to calculate the loss function, $L_p(T) = -(1/N_p) \times (dT/dx)$, where

$$-\frac{dT}{dx} = \frac{\omega_p^2 e^2}{v^2}\ln\frac{mv^3}{\gamma_0 e^2\omega_p} \quad \text{for } kT_e \ll T \ll 14.6 \text{ eV}, \quad (20)$$

$$-\frac{dT}{dx} = \frac{\omega_p^2 e^2}{2v^2}\left(\ln\frac{mv^2T}{I_e^2} + 1 - [2(1-\beta^2)^{1/2}+\beta^2]\ln 2 + \frac{1}{8}[1-(1-\beta^2)^{1/2}]^2\right) \quad \text{for } T \geqslant 14.6 \text{ eV}, \quad (21)$$

and ω_p is the plasma frequency $[=(4\pi N_p e^2/m)^{1/2}]$, $\ln\gamma_0$ is Euler's constant (0.577), T_e is the electron temperature, and I_e is an average excitation energy of the plasma electrons

given in terms of the dielectric function of the electron gas, $\epsilon_e(\omega)$, as

$$\ln I_e = \frac{2}{\pi\omega_p^2}\int_0^\infty \omega\,\mathrm{Im}[-\epsilon_e(\omega)^{-1}]\ln\hbar\omega\,d\omega. \quad (22)$$

In the limit of nonrelativistic energies, small damping[53] ($I_e \simeq \hbar\omega_p$), and $N_p \ll 1.6\times10^{24}$ cm^{-3}, Eq. (21) reduces to the high-energy, nonrelativistic equation given by Perkins.[52] The cutoff energy, 14.6 eV, is chosen to ensure continuity between Eqs. (20) and (21).

In Eq. (1), the ionization fraction, N_p/N_0, is entered as a parameter. For nonrelativistic energies, Dalgarno and Lejeune[4] and Slinker and co-workers[10] analyzed the sensitivity of their oxygen deposition model to changes in the fractional ionization. Similar results are presented in the next section.

III. RESULTS

The discrete energy deposition scheme described above and in paper I is utilized for beam electrons with energies ranging from 100 eV to 10 MeV. For all cases, the beam flux was fixed at 1.99×10^{18} cm^{-2} s^{-1} and the background gas densities at 2.46×10^{19} cm^{-3}. This beam flux corresponds to a uniform cylindrical beam with a 1-cm radius and 1-A current. If the plasma loss term is ignored, Eqs. (1) and (2) show that the equilibrium distribution function is proportional to the beam flux and independent of the background density for a single species gas. In this case, the background density simply scales the time. Unless otherwise noted, the fractional ionization was zero. The quantities defined below are also defined in paper I. Results for deposition in N and N^+ are discussed in this section.

The total inelastic cross section, $\sigma(T)$, contains contributions from electron-impact excitation, σ_e, and ionization, σ_i, and is given by

$$\sigma(T) = \sigma_e(T) + \sigma_i(T) = \sum_j \sigma_j(T) + \sum_i \sigma_i(T). \quad (23)$$

Using the information presented in Secs. II B–II E, these cross sections are shown in Fig. 1 for energies up to 10 MeV. A comparison of Fig. 1(a) for N with Fig. 1(b) for N^+ shows the different threshold behaviors described earlier. For energies greater than 1 MeV, the relativistic rise is apparent.

The loss function accounts for energy loss to excitation, $L_e(T)$, and ionization, $L_i(T)$, as well as energy carried away by secondary electrons, $L_s(T)$, and may be written as

$$L(T) = L_e(T) + L_i(T) + L_s(T) = \sum_j E_j\sigma_j(T) + \sum_i I_i\sigma_i(T) + \sum_i \int_0^{(T-I_i)/2} \epsilon\sigma_i'(T,\epsilon)\,d\epsilon. \quad (24)$$

Figure 2 shows $L(T)$ and its components for energies up to 10 MeV for both N and N^+. In both cases, most of the energy goes into producing secondary electrons above several hundred eV, while loss to excitation is significant only below

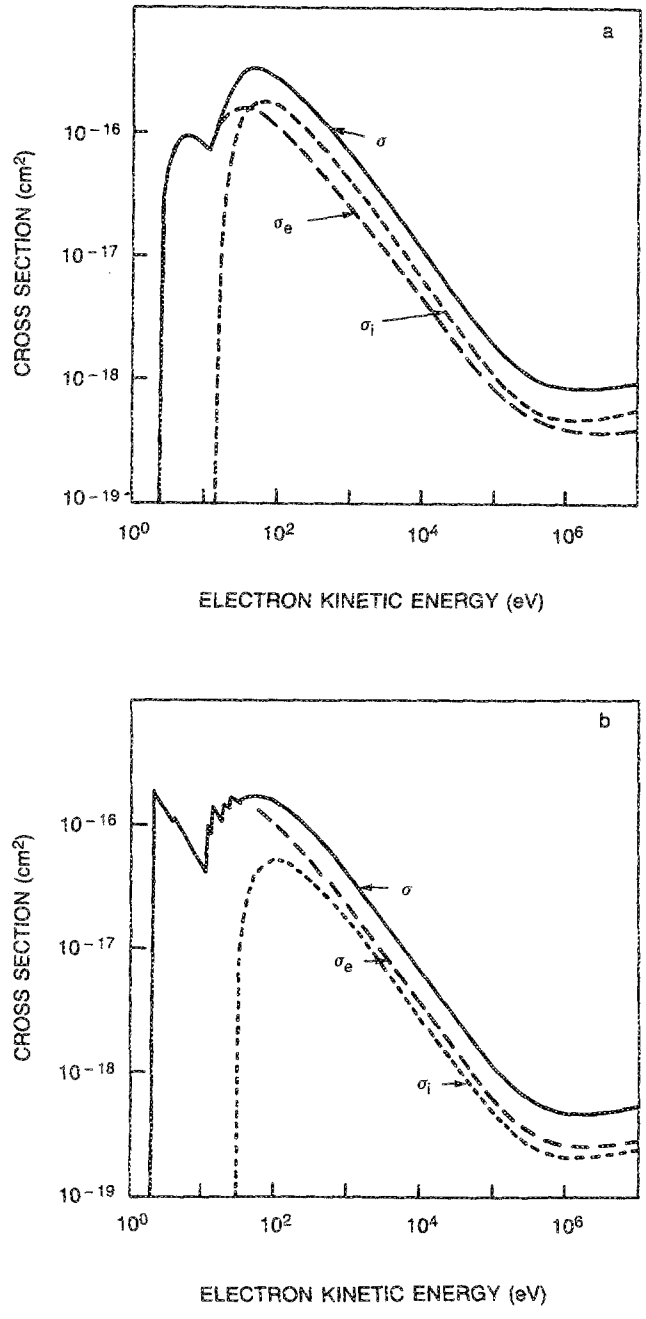

FIG. 1. Total excitation (long dashes), total ionization (short dashes), and total inelastic (solid line) cross sections for (a) N and (b) N^+.

the ionization threshold. Figure 2 also shows a comparison between $L(T)$ and Bethe's relativistic loss function,[23]

$$L_B(T) = \frac{2\pi r_e^2 mc^2}{\beta^2} Z\left[\log\left(\frac{T^2}{I_0^2}\frac{(\gamma+1)}{2}\right) + \frac{1}{\gamma^2} - \frac{2\gamma-1}{\gamma^2}\log 2 + \frac{1}{8}\left(\frac{\gamma-1}{\gamma}\right)^2\right]. \quad (25)$$

In Eq. (25), $Z = 7$ for N and N^+, r_e is the classical electron radius, I_0 is a mean excitation energy ($I_0 = 85.0$ for nitrogen[54]), and $\gamma = (1-\beta^2)^{-1/2}$. For N, $L(T)$ and $L_B(T)$ are in close agreement at energies greater than 1 keV; for N^+, agreement is good above 10 keV. The energy loss of an elec-

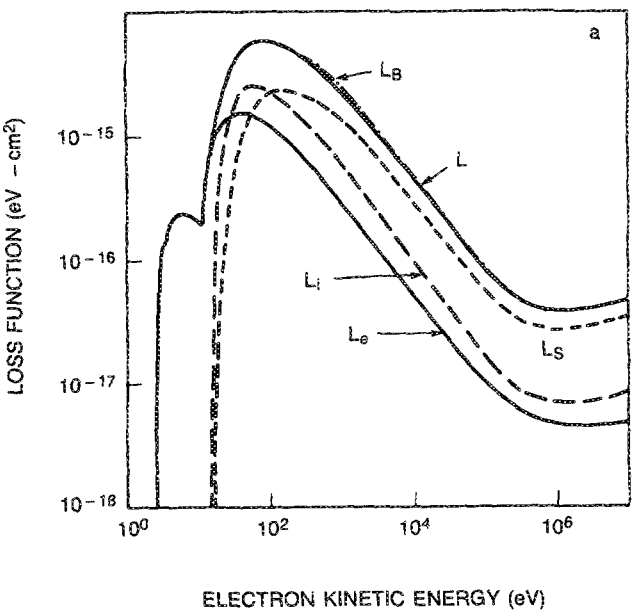

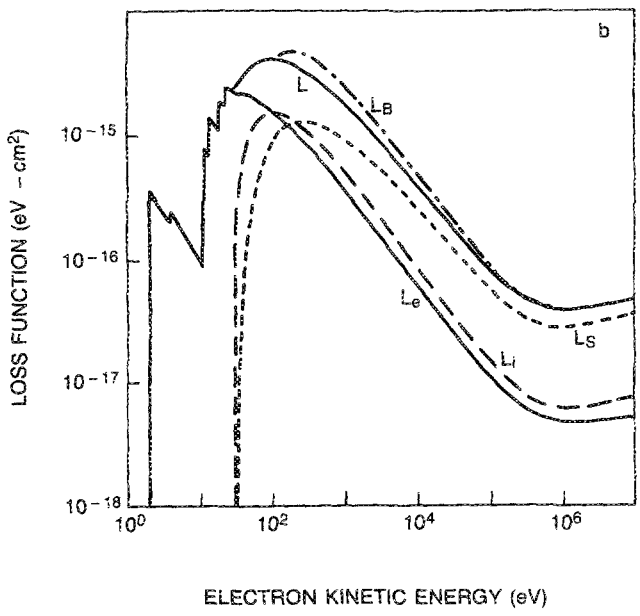

FIG. 2. Total loss function (solid line) partitioned into excitation (lower solid line), ionization (long dashes), and secondary electron (short dashes) contributions and compared to Bethe's formula, Eq. (25) (dash-dotted line) for (a) N and (b) N^+.

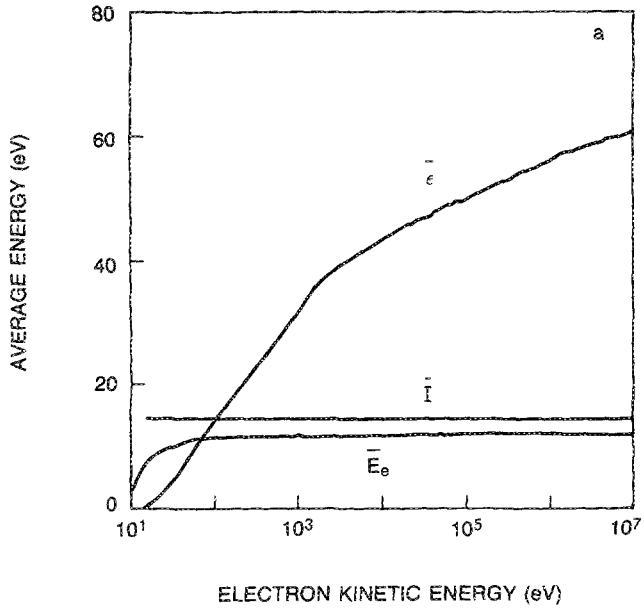

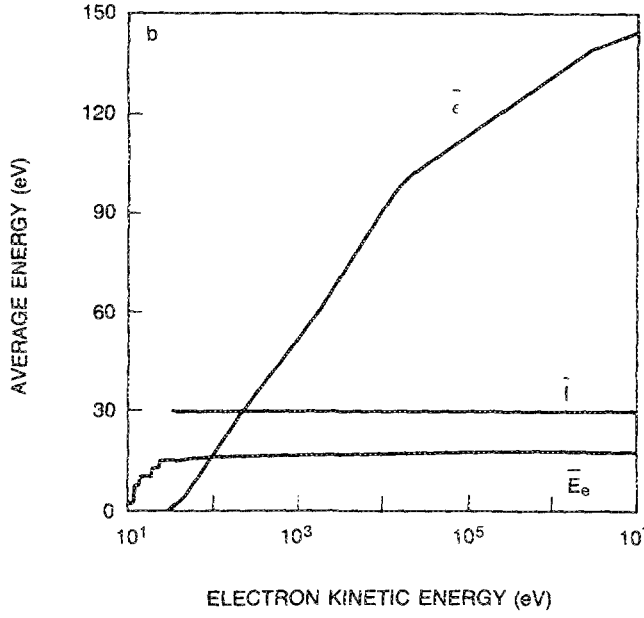

FIG. 3. Average excitation, ionization, and secondary energies defined according to Eqs. (26)–(28) for (a) N and (b) N^+.

tron traversing a material is lessened because of polarization of the medium.[54–56] The magnitude of this effect depends not only on the electron energy, but also on the gas density (which is on the order of atmospheric density in this case). This density effect is small for the energies in the present studies and, therefore, has not been included.

Average excitation ($\bar{E}_e$), ionization ($\bar{I}$), and secondary ($\bar{\epsilon}$) energies (per event) are defined as

$$E_e \equiv L_e(T)/\sigma_e(T), \tag{26}$$

$$\bar{I} \equiv L_i(T)/\sigma_i(T), \tag{27}$$

$$\bar{\epsilon} \equiv L_s(T)/\sigma_i(T), \tag{28}$$

and shown in Fig. 3. There is very little change in $\bar{I}$ and $\bar{E}_e$ for energies greater than ~ 100 eV. Asymptotically, $\bar{I} = 14.5$ eV and $\bar{E}_e = 11.9$ eV for N and $\bar{I} = 29.7$ eV and $\bar{E}_e = 17.8$ eV for N^+. These averages also show how most of the energy in a typical collision goes into producing secondaries. For N, a simple scaling relation, with an accuracy of better than 4%, for the average energy of the secondary electron as a function of the incident primary energy is

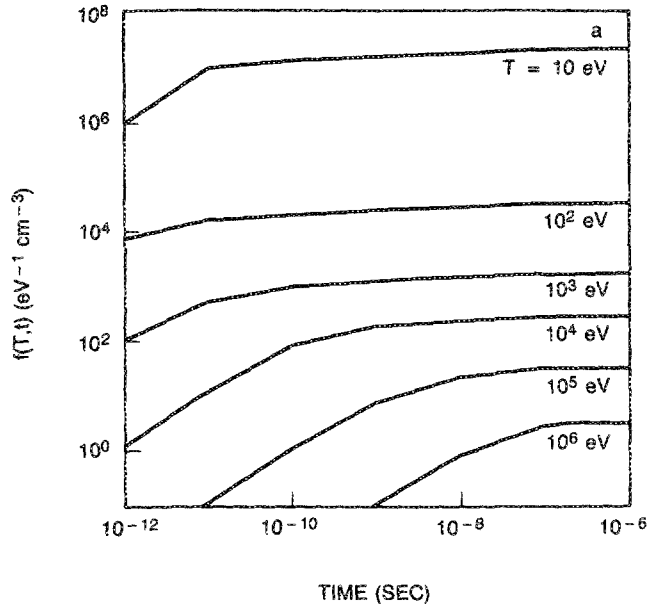

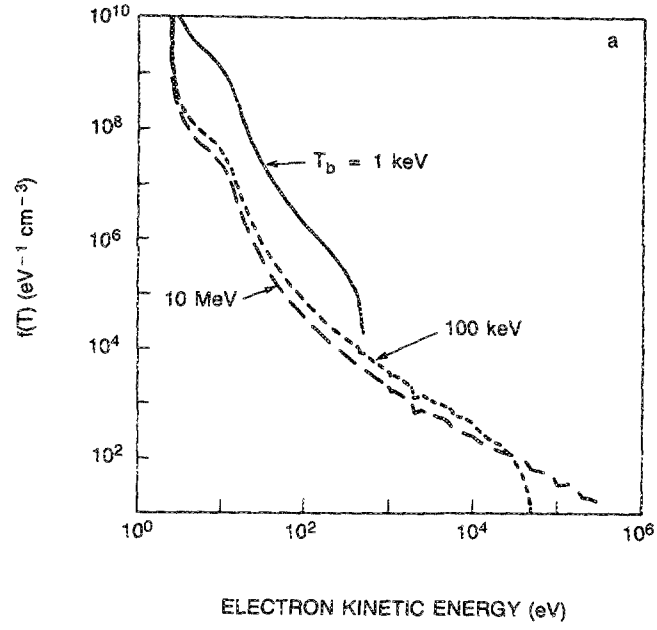

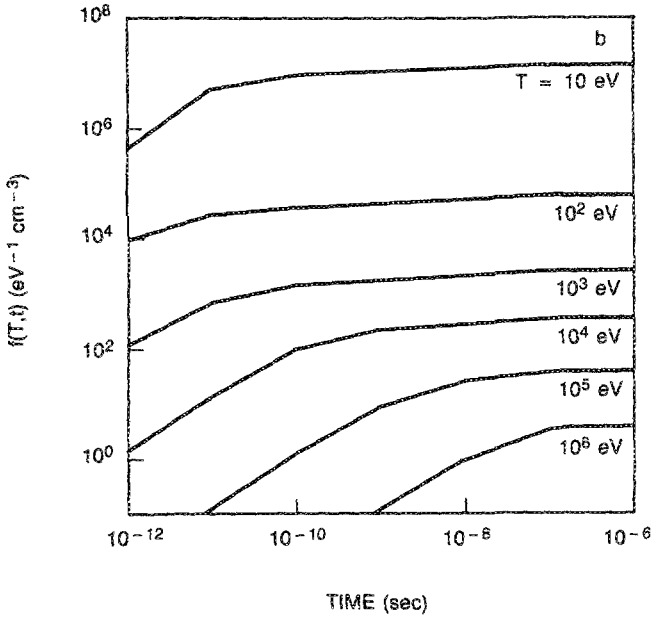

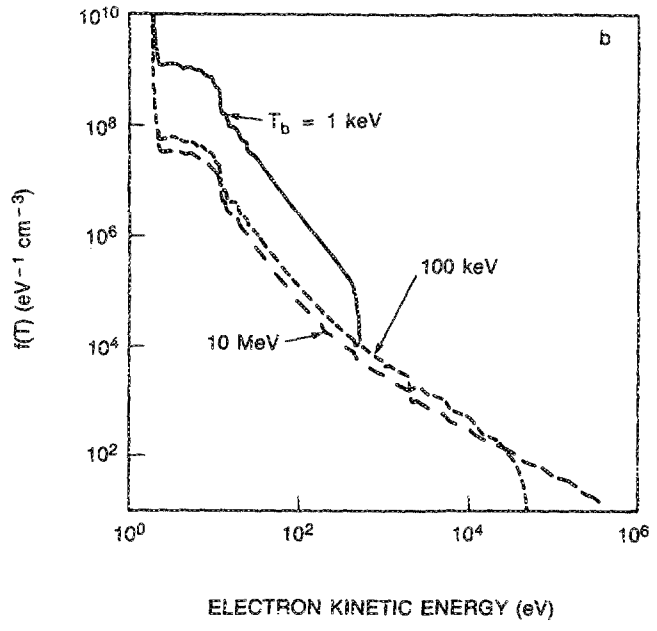

FIG. 4. Relaxation of $f(T,t)$ to steady state for $T = 10^1$–10^6 eV for a 10 MeV beam on (a) N and (b) N^+. The gas densities were fixed at 2.46×10^{19} cm^{-3}.

FIG. 5. Steady-state distribution function, $f(T)$, for beam energies of 1 keV (solid line), 100 keV (short dashes), and 10 MeV (long dashes) for (a) N and (b) N^+.

$$\bar{\epsilon} = 7.93(\ln T - 2.88) \quad \text{for } 100\text{ eV} \leqslant T \leqslant 3\text{ keV}, \quad (29)$$

$$\bar{\epsilon} = 2.75(\ln T + 6.78) \quad \text{for } 3\text{ keV} \leqslant T \leqslant 10\text{ MeV}. \quad (30)$$

For N^+, the scaling relation, with a 3% accuracy, is

$$\bar{\epsilon} = 16.19(\ln T - 3.59) \quad \text{for } 50\text{ eV} \leqslant T \leqslant 20\text{ keV}, \quad (31)$$

$$\bar{\epsilon} = 7.53(\ln T + 3.67) \quad \text{for } 20\text{ keV} \leqslant T \leqslant 10\text{ MeV}. \quad (32)$$

The time-dependent Boltzmann equation was solved using numerical methods discussed in the Appendix of paper I. The distribution function $f(T,t)$ is observed to relax to a steady-state solution $f(T)$. For a 10-MeV beam on N and N^+, this relaxation is shown in Fig. 4. The characteristic relaxation time is energy dependent, i.e. relaxation is nonuniform. Intermediate energies ($\sim$100 eV) relax first, followed by the lower part of the spectrum ($\sim$10 eV, but greater than the lowest excitation energy), and, finally, the high energies ($\geqslant$1 keV). Similar observations were made by Bretagne *et al.*[14] for Ar and in paper I for oxygen. Figure 5 shows steady-state distribution functions for several beam energies. The apparent structure for $T \geqslant 1$ keV is nonphysical and a direct consequence of the choice of grid. Changing the grid changes the structure. Choosing a finer grid results in no structure, but drastically increases both computer time and memory required to obtain the results. In Fig. 5(b), the

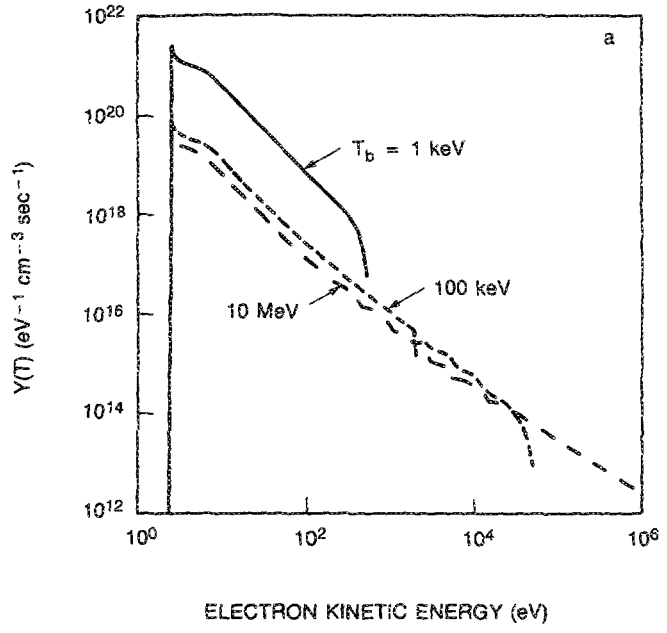

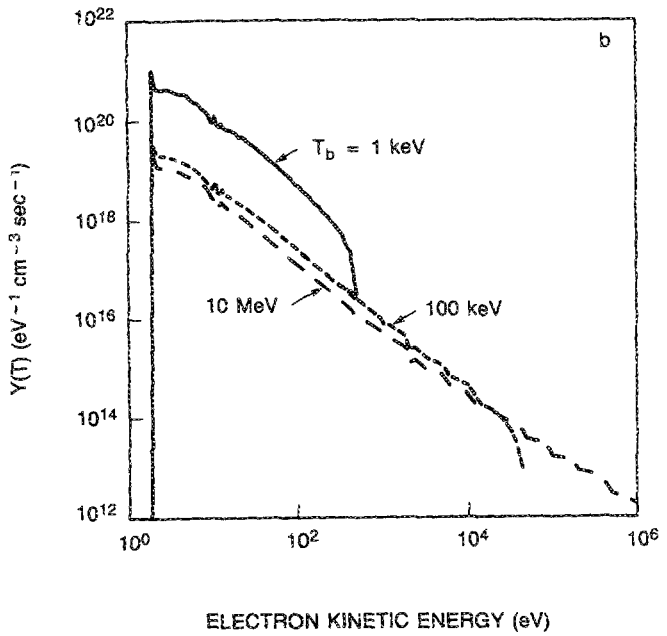

FIG. 6. Yield spectra, $Y(T)$, for beam energies of 1 keV (solid line), 100 keV (short dashes), and 10 MeV (long dashes) for (a) N and (b) N^+.

structure for $T \leqslant 30$ eV is related to the structure in the cross section seen in Fig. 1(b).

Yield spectra, $Y(T)$ [$= N_0 \sigma(T) v(T) f(T)$], are shown in Fig. 6. These are proportional to similar quantities analyzed by Green and co-workers.[5,20,21] For completely stopped source electrons (from 50 eV to 10 keV), Green, Jackman, and Garvey[5] find that the yield functions fall off with energy as $T^{-1.58}$ for any source energy. Our oxygen results[10] show that the T dependence for $Y(T)$ is independent of T_b for beam sources as well. This result was also found by Garvey, Porter, and Green[20,21] for H_2 and beam energies up to 10 MeV. For N and N^+, the yield spectra show this energy behavior. Specifically, we find that the yield spectra are well approximated by

$$Y(T) = F(T_b) G(T), \tag{33}$$

where

$$F(T_b) = (1/2\pi r_e^2 mc^2 Z) L_B(T_b) \tag{34}$$

and

$$G(T) = (\alpha/T^{\delta})\Theta(T_c - T) + (\eta/T^{\zeta})\Theta(T - T_c). \tag{35}$$

In Eq. (35), α, δ, η, ζ, and T_c are parameters and Θ is the Heaviside step function. Using the parameters in Table VI, Eqs. (33)–(35) give good fits to the yield spectra for a large range of T_b (1 keV–10 MeV) and T (1 eV–10 MeV). Representative "worse case" (10 keV) and "best case" (1 MeV) results are shown in Fig. 7. The largest discrepancy is for the high T tail when $T_b \leqslant 10$ keV. Equations (33) and (34) suggest that $f(T)$ is proportional to the loss function, $L_B(T_b)$. Bretagne *et al.*[14] found a similar dependence for electron distributions in an electron-beam-generated argon plasma.

As mentioned previously, the energy necessary to produce an electron-ion pair, W, is particularly useful for simplifying the description of ionization in a gas. For beam sources, it is given by

$$W = \frac{N_0 N_b(T_b) v(T_b) L(T_b)}{\int S(T) dT + \Sigma_i N_0 \int \sigma_i(T) v(T) f(T,t) dT}, \tag{36}$$

where the first term in the denominator gives the rate for producing electron-ion pairs directly by beam ionization and the second term is the production rate for all generations of secondaries. Equation (36) shows that W is, in general, a time-dependent function, through its dependence on $f(T,t)$. The steady-state values are obtained by replacing $f(T,t)$ with $f(T)$ and may be calculated, for a given beam energy, according to

$$W = \bar{E}(T_b)/\bar{N}(T_b), \tag{37}$$

where

$$\bar{E}(T_b) = \bar{I}(T_b) + \epsilon(T_b) + \bar{E}_e(T_b)[\sigma_e(T_b)/\sigma_i(T_b)], \tag{38}$$

and

TABLE VI. Parameters for analytic fits to the yield spectra.

N parameters				
α	δ	η	ζ	T_c
7.81×10^{18}	1.585	1.26×10^{18}	1.234	2.00×10^{2}
N^+ parameters				
α	δ	η	ζ	T_c
2.53×10^{18}	1.361	3.44×10^{17}	1.150	1.4×10^{4}

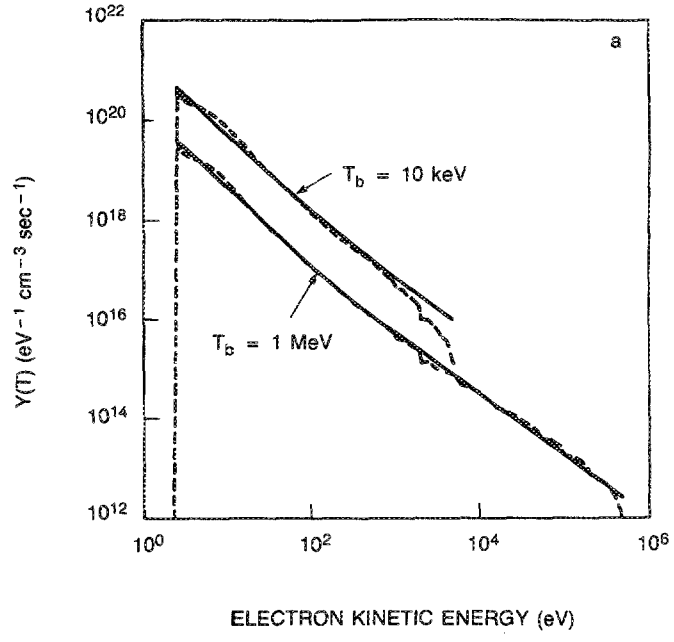

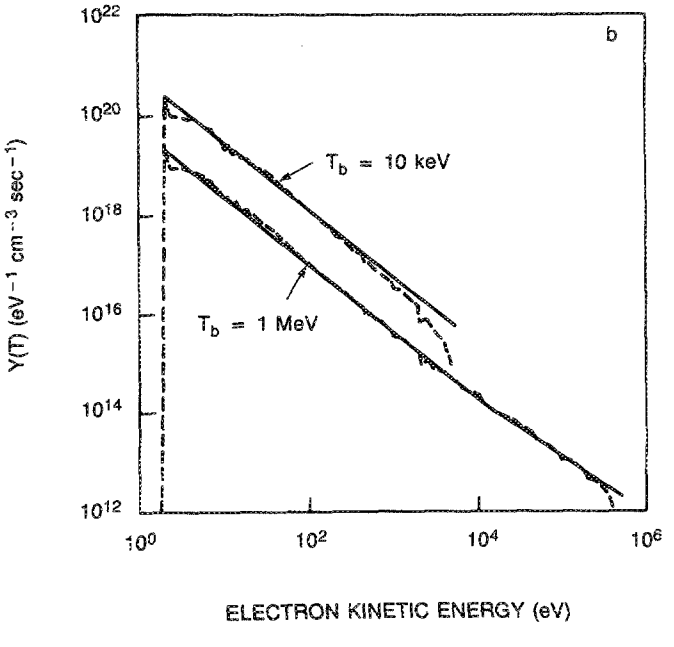

FIG. 7. Yield spectra (dashed lines) and analytic fits (solid lines) for beam energies of 10 keV and 10 MeV for (a) N and (b) N^+.

$$\bar{N}(T_b) = 1 + [N_0\Phi_b(T_b)\sigma_i(T_b)]^{-1} \times \int_I^{T_b/2} Y(T)\left(1 + \frac{\sigma_e(T)}{\sigma_i(T)}\right)^{-1} dT. \quad (39)$$

In Eq. (39) Φ_b is the beam flux, $N_b v(T_b)$. The steady-state values of W for beam energies ranging from 100 eV to 10 MeV are shown in Table VII. These values are nearly constant over the entire energy range. The near constancy of W at energies $\geqslant 100$ eV is well-known.[20,57-62] Fano[58] attributes this result to the fact that the ratios of the excitation and ionization cross sections are insensitive to energy. For N and N^+ deposition, σ_e/σ_i is only approximately constant for 1 keV $\leqslant T_b \leqslant$ 10 MeV. For N, this ratio varies between 0.59 and 0.81, i.e., a variation of 16% about the mean. A 3% variation occurs for N^+, specifically σ_e/σ_i is between 1.19 and 1.26. However, as pointed out below, this fact alone does not seem sufficient to explain the constancy of W. Inokuti[59] and Spencer[62] have utilized the constancy of W to develop useful analytic models for their yield functions. Garvey and coworkers[20] use a polynomial fit for their yield spectra to demonstrate that, to first order, W is independent of the source energy. Although the leading term in their expansion for W is a constant, it does not reproduce their computed value of W with any degree of accuracy and, thus, does not provide an accurate demonstration of this constancy.

TABLE VII. W vs electron-beam energy, T_b, for N and N^+.

	N results					
T_b (eV)	10^2	10^3	10^4	10^5	10^6	10^7
W (eV)	30.9	30.8	31.0	31.4	31.4	30.8
	N^+ results					
T_b (eV)	10^2	10^3	10^4	10^5	10^6	10^7
W (eV)	76.0	71.2	72.3	72.5	72.1	71.1

Following an analysis similiar to that of Garvey, Porter, and Green,[20] we can obtain an expansion for W in terms of T_b. By substituting Eqs. (33)–(35) into (37)–(39), assuming $L(T_b) \simeq L_B(T_b)$ for $T_b > 1$ keV, and letting $\kappa = (2\pi r_e^2 mc^2 Z N_0 \Phi_b)$, Eq. (39) becomes

$$\bar{N}(T_b) = 1 + \kappa \bar{E}(T_b)\Gamma(T_b). \quad (40)$$

If σ_e/σ_i is assumed constant for $T \geqslant T_c$ (a better assumption for N^+ than N), then

$$\Gamma(T_b) = \Gamma_\infty - A/T^{\zeta-1}, \quad (41)$$

where

$$A = 2^{\zeta-1}[\eta/(\zeta-1)][1 + \sigma_e(T_c)/\sigma_i(T_c)]^{-1}, \quad (42)$$

and Γ_∞ is evaluated numerically. Γ_∞ is dominated by low T yield with some high T contribution. The second term in Eq. (41) is due exclusively to the high T yield. For the cases considered here, $\kappa\bar{E}\,\Gamma$ is of the order of unity. Expanding about $\kappa\bar{E}\,\Gamma = 1$ and letting $x = \kappa\bar{E}\,\Gamma - 1$ gives,

$$W = \left(\frac{\bar{E}}{2}\right)\left(1 - \frac{x}{2} + \frac{x^2}{4} - \frac{x^3}{8} + \cdots\right). \quad (43)$$

To reproduce the computed values of W (see Table VII), to within 4%, the first four terms must be retained in the expansion. The constancy of W cannot be demonstrated or explained by extracting only a leading constant term from Eq. (43). When Eqs. (38) and (40)–(42) are used to calculate W, substantial errors result if the high T component of

the yield spectra is not fitted accurately. Our observation is that W is approximately constant for beam energies between 1 keV and 10 Mev because $\overline{E}$ and $\overline{N}$, as calculated exactly, i.e., by Eqs. (38) and (39), increase by approximately the same amount and at approximately the same rate.

For a given state the production efficiency, $P_j(T_b)$, is defined as the number of excitations of that state per electron-ion pair created, i.e.,

$$P_j(T_b) = \frac{N_0 \int \sigma_j(T) v(T) f(T,t) dT + N_0 \sigma_j(T_b) v(T_b) N_b(T_b)}{N_0 N_b(T_b) v(T_b) L(T_b)/W} . \tag{44}$$

For a 10-MeV beam on N, the six largest production efficiencies are given in Table VIII. These production efficiencies are nearly constant for beam energies of 100 eV to 10 MeV. The production efficiency for the single ionization continuum is unity.

The results discussed above depend, in part, on the value of the assumed ionization fraction.[4] The sensitivity of these results has been investigated. In particular, Fig. 8 shows that the distribution function, $f(T)$, for N in assumed fractional backgrounds between 0.0 and 0.01 and for N^+ where the background varies from 0.0 to 1.0. The N results are similiar to those obtained in paper I for oxygen, i.e., $f(T)$ is insensitive to changes in the background ionization for energies greater than ~ 30 eV, but highly sensitive for lower energies. Table IX shows W and the percentage of deposition energy lost to the background electrons for various ionization fractions. While energy loss increases with increasing numbers of background electrons, W remains nearly constant for N until the fraction approaches 10^{-2}. When N^+ is present in significant amounts in electron-beam experiments, the background electron density is generally the same order of magnitude. For this reason, the ionization fraction for N^+ was varied from 0.0 to 1.0. $f(T)$ shows a sensitivity at all energies while W changes dramatically for fractions greater than 0.05.

IV. SUMMARY

A discrete model has been used to study energy deposition by relativistic electron beams in N and N^+. For beam energies between 100 eV and 10 MeV, the energy required to produce an electron-ion pair is approximately 31 eV in N and 72 eV in N^+. For a 10-MeV beam on N, W is approximately constant for background ionization fractions between 0.0 and 10^{-3}. The production efficiencies also remain nearly constant over most of the energy range. The time-dependent model is used to observe the nonuniform

TABLE VIII. Production efficiencies for a 10-MeV beam on N.

State	P_j	State	P_j
$^2D^0 2p^3$	1.55	^4P 3p	0.13
$^2P^0 2p^3$	0.35	^4P 3d	0.11
^4P 3s	0.32		
$^4P 2s2p^4$	0.14	$N^+(^3P)$	1.0

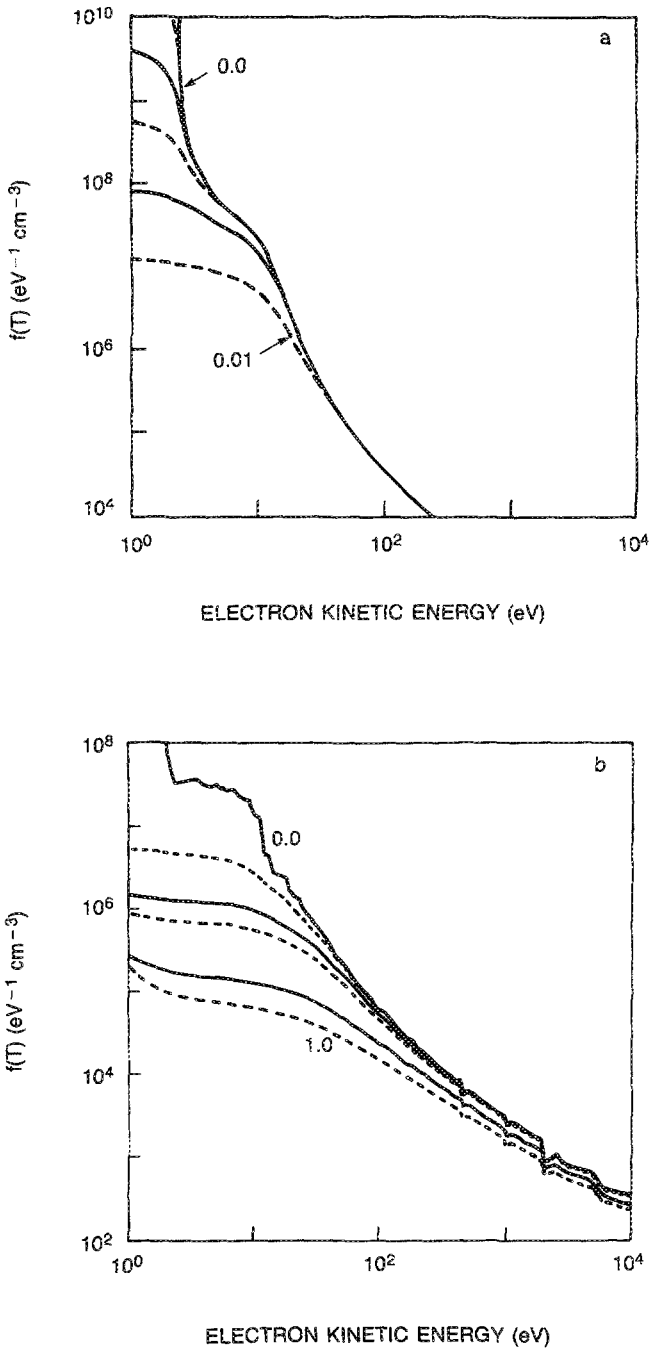

FIG. 8. $f(T)$ for fractional ionizations of (a) 0.0, 10^{-6}, 10^{-5}, 10^{-4}, 10^{-3}, and 10^{-2} (from top to bottom) for N and (b) 0.0, 0.01, 0.05, 0.1, 0.5, and 1.0 (from top to bottom) for N^+.

TABLE IX. W and energy loss to plasma electrons versus ionization fraction for N and N^+.

	N results					
Fraction	0.0	10^{-6}	10^{-5}	10^{-4}	10^{-3}	10^{-2}
W (eV)	30.8	30.8	30.8	30.8	30.9	31.8
Energy loss (%)	0.0	3.5	4.0	5.9	11.9	22.0
	N^+ results					
Fraction	0.0	0.01	0.05	0.1	0.5	1.0
W (eV)	71.1	72.3	75.7	79.0	94.8	106.6
Energy loss (%)	0.0	12.4	22.0	27.6	43.3	50.4

relaxation of the secondary electron distribution to a steady-state solution.

ACKNOWLEDGMENTS

This work was supported by the Defense Advanced Research Projects Agency under ARPA Order No. 4395, Amendment No. 63, and monitored by the Naval Surface Weapons Center.

[1]U. Fano, Phys. Rev. **92**, 328 (1953).
[2]L. V. Spencer and U. Fano, Phys. Rev. **93**, 1172 (1954).
[3]M. Inokuti, in *Applied Atomic Collision Physics*, edited by S. Datz (Academic, New York, 1983), Vol. 4.
[4]A. Dalgarno and G. Lejeune, Planet. Space Sci. **19**, 1653 (1971).
[5]A. E. S. Green, C. H. Jackman, and R. H. Garvey, J. Geophys. Res. **82**, 5104 (1977).
[6]P. S. Ganas and A. E. S. Green, J. Quant. Spectrosc. Radiat. Transfer **25**, 265 (1981).
[7]R. P. Singhal and A. E. S. Green, J. Geophys. Res. **86**, 4776 (1981).
[8]D. J. Strickland and A. W. Ali, "A Code for the Secondary Electron Energy Distribution in Air and Some Applications," NRL Memorandum Report 4956, Washington, DC (1982).
[9]S. Slinker and A. W. Ali, "Electron Energy Deposition in Atomic Oxygen," NRL Memorandum Report 5909, Washington, DC (1986).
[10]S. P. Slinker, R. D. Taylor, and A. W. Ali, J. Appl. Phys. **63**, 1 (1988).
[11]R. D. Taylor, S. P. Slinker, and A. W. Ali, "Electron Energy Deposition in Atomic Nitrogen," NRL Memorandum Report 6087, Washington, DC (1987).
[12]S. D. Rockwood, Phys. Rev. A **8**, 2348 (1973).
[13]S. D. Rockwood, J. E. Brau, W. A. Proctor, and G. H. Caravan, IEEE J. Quantum Electron. **9**, 120 (1973).
[14]J. Bretagne, G. Delouya, J. Godart, and V. Puech, J. Phys. D **14**, 1225 (1981).
[15]A. E. S. Green and C. A. Barth, J. Geophys. Res. **70**, 1083 (1965).
[16]A. E. S. Green and C. A. Barth, J. Geophys. Res. **72**, 3975 (1967).
[17]R. S. Stolarski and A. E. S. Green, J. Geophys. Res. **72**, 3967 (1967).
[18]L. R. Peterson, Phys. Rev. **187**, 105 (1969).
[19]H. S. Porter, C. H. Jackman, and A. E. S. Green, J. Chem. Phys. **65**, 154 (1976).
[20]R. H. Garvey, H. S. Porter, and A. E. S. Green, J. Appl. Phys. **48**, 4353 (1977).
[21]R. H. Garvey, H. S. Porter, and A. E. S. Green, J. Appl. Phys. **48**, 190 (1977).
[22]Y. A. Medvedev and V. D. Khokhlov, Sov. Phys. Tech. Phys. **24**, 181 (1979); *ibid* 185 (1979).
[23]H. A. Bethe, *Handbuch der Physik* (Springer, Berlin, 1933), Vol. 24, p. 273.
[24]R. W. Schunk and P. B. Hayes, Planet. Space Sci. **19**, 113 (1971).
[25]R. D. Taylor and A. W. Ali, "Excitation and Ionization Cross Sections for Electron-Beam Energy Deposition in High Temperature Air," NRL Memorandum Report 6013, Washington, DC (1987).
[26]H. W. Drawin, "Collision and Transport Cross Sections," Report EUR-CEA-FC-383, Fontenay-aux-Roses (1966) and revised (1967).
[27]H. Bethe, Z. Phys. **76**, 293 (1932).
[28]For an excellent discussion of the Bethe theory for inelastic collisions of fast charged particles with atoms see M. Inokuti, Rev. Mod. Phys. **43**, 297 (1971) and M. Inokuti, Y. Itikawa, and J. Turner, Rev. Mod. Phys. **50**, 23 (1978).
[29]W. L. Wiese, M. W. Smith, and B. M. Glennon, *Atomic Transition Probabilities*, NSRDS-NBS4 (U. S. Government Printing Office, Washington, DC, 1966), Vol. 1.
[30]N. F. Mott and H. S. W. Massey, *The Theory of Atomic Collisions*, 3rd ed. (Clarendon, Oxford, 1965).
[31]L. R. Peterson, S. S. Prasad, and A. E. S. Green, Can. J. Chem. **47**, 1774 (1969).
[32]A. E. S. Green and S. K. Dutta, J. Geophys. Res. **72**, 3933 (1967).
[33]A. E. S. Green and R. S. Stolarski, J. Atmos. Terr. Phys. **34**, 1703 (1972).
[34]A. E. S. Green and T. Sawada, J. Atmos. Terr. Phys. **34**, 1719 (1972).
[35]C. H. Jackman, R. H. Garvey, and A. E. S. Green, J. Geophys. Res. **82**, 5081 (1977).
[36]R. H. Neynaber, L. L. Marino, E. W. Rothe, and S. M. Trujillo, Phys. Rev. **129**, 2069 (1963).
[37]R. J. W. Henry, P. G. Burke, and A. -L. Sinfailam, Phys. Rev. **178**, 218 (1969).
[38]S. Ormonde, K. Smith, B. W. Torres, and A. R. Davies, Phys. Rev. A **8**, 262 (1973).
[39]K. A. Berrington, P. G. Burke, and W. D. Robb, J. Phys. B **8**, 2500 (1975).
[40]A. T. Jusick, C. E. Watson, L. R. Peterson, and A. E. S. Green, J. Geophys. Res. **72**, 3943 (1967).
[41]M. Van Regermorter, Astrophys. J. **136**, 906 (1962).
[42]M. J. Seaton, in *Atomic and Molecular Processes*, edited by D. R. Bates (Academic, New York, 1962).
[43]L. A. Vainstein, Opt. Spectrosc. **14**, 163 (1961).
[44]A. Burgess, Mem. Soc. R. Liege Collect. **4**, 299 (1961).
[45]P. S. Ganas, J. Chem. Phys. **72**, 2197 (1980).
[46]H. E. Saraph, M. J. Seaton, and J. Shemming, Proc. R. Soc. London **89**, 27 (1966).
[47]E. J. McGuire, Phys. Rev. A **3**, 267 (1971).
[48]E. Brook, M. F. Harrison, and A. C. H. Smith, J. Phys. B **11**, 3115 (1978).
[49]M. Inokuti, M. Dillon, J. Miller, and K. Omidvar, J. Chem. Phys. **87**, 6967 (1987).
[50]M. F. A. Marrison, K. T. Dolder, and P. C. Thonemann, Proc. Phys. Soc. **82**, 368 (1963).
[51]E. J. McGuire, Phys. Rev. **25**, 192 (1982).
[52]F. Perkins, Phys. Fluids **8**, 1361 (1965).
[53]V. N. Tsytovich, Zh. Eksp. Teor. Fiz. **42**, 803 (1962) [Sov. JETP **15**, 561 (1962)]; R. J. Gould, Physica (Utr.) **60**, 145 (1972); L. Vriens, Phys. Rev. A **8**, 332 (1973).
[54]L. Pages, E. Bertel, H. Joffre, and L. Sklavenitis, At. Data **4**, 1 (1972).
[55]E. Fermi, Phys. Rev. **57**, 485 (1940).
[56]R. M. Sternheimer, Phys. Rev. **145**, 247 (1966).
[57]A. Dalgarno, in *Atomic and Molecular Processes*, edited by D. R. Bates (Academic, New York, 1962).
[58]U. Fano, Phys. Rev. **70**, 44 (1946).
[59]M. Inokuti, Radiat. Res. **64**, 6 (1975).
[60]U. Fano and L. V. Spencer, Int. J. Radiat. Phys. Chem. **7**, 63 (1975).
[61]D. A. Douthat, Radiat. Res. **64**, 141 (1975).
[62]L. V. Spencer, Radiat. Res. **97**, 219 (1984).